Available online at www.sciencedirect.com
SCIENCE DIRECT®
ELSEVIER
Nuclear Instruments and Methods in Physics Research A 532 (2004) 371–375
NUCLEAR INSTRUMENTS & METHODS IN PHYSICS RESEARCH Section A
www.elsevier.com/locate/nima

MD simulation of beam ordering

H. Tsutsui[a,*], T. Katayama[b], I. Meshkov[c], A. Sidorin[c], A. Smirnov[c], E. Syresin[c], D. Möhl[d]

[a] Research and Development Center, Sumitomo Heavy Industries, Ltd., 2-1-1 Yato, Nishitokyo, Tokyo 188-8585, Japan
[b] Beam Physics and Engineering Laboratory, RIKEN, 2-1 Hirosawa, Wako, Saitama 351-0198, Japan
[c] LNP JINR, 6 Joliot Curie, Dubna 141980, Russia
[d] PS Division, CERN, CH-1211 Geneva 23, Switzerland

Available online 28 July 2004

Abstract

A molecular dynamics simulation code using a second-order symplectic integral method is presented. This code is applied to ESR experiments of 1D crystalline beam, and the simulations reproduce the sudden reduction of the momentum spread. Some conditions for obtaining 1D crystalline state are discussed.

PACS: 29.27.−a; 41.75.−i

Keywords: Crystallization; MD simulation; Symplecticity

1. Introduction

When an ion beam in a synchrotron is extremely cooled, the ions are aligned on one-, two-, or three-dimensional lattice, according to the balance of the repelling Coulomb force. The experimental possibilities of heavy ion storage ring projects such as MUSES [1] can be enhanced if this ordered state is achieved. In order to design an ion ring optimized for these experiments, a simulation code was developed, which is described in Section 2. In Section 3, the code is applied to the ESR experiments [2,3]. Some conditions necessary to achieve 1D crystalline state are discussed in Section 4.

2. Symplectic MD simulation code

The Hamiltonian of our molecular dynamics (MD) simulation code is [5]

$$H = H_0 + H_{\mathrm{sc}}$$

$$H_0 = -\frac{xp_z}{\rho(s)} + \frac{p_z^2}{2\gamma_0^2} + \frac{p_x^2 + p_y^2}{2} + \left(\frac{1}{\rho(s)^2} + K(s)\right)\frac{x^2}{2} - \frac{K(s)}{2}y^2$$

*Corresponding author.
E-mail address: htsutsui@postman.riken.go.jp (H. Tsutsui).

0168-9002/$ - see front matter © 2004 Elsevier B.V. All rights reserved.
doi:10.1016/j.nima.2004.06.066

$$H_{\rm sc} = \frac{r_{\rm ion}}{\gamma_0^2\beta_0^2}\sum_{i=1}^{N}\left[(x-x_i)^2+(y-y_i)^2 + \gamma_0^2(z-z_i)^2\right]^{-1/2} \quad (1)$$

where $\mathbf{r}=(x,y,z)$, $\mathbf{p}=(p_x,p_y,p_z=\Delta p/p)$, $\rho(s)$, γ_0, β_0, $K(s)$, and $r_{\rm ion}$ are the coordinate, canonical momentum, curvature radius, relativistic factor, normalized velocity, quadrupole field strength, and classical radius of ion, respectively.

A transfer map $\mathscr{M}$ from a function on s_2 to a function on s_1 is approximated as

$$\begin{aligned}\mathscr{M} &\equiv T\exp\left(-\int_{s_1}^{s_2} {\rm d}s' : H(s') :\right)\\ &\approx \prod_i\left[\exp\left(-:\frac{H_0(s_i)\Delta s_i}{2}:\right)\right.\\ &\quad\times \exp(-:H_{\rm sc}(s_i)\Delta s_i:)\\ &\quad\left.\times \exp\left(-:\frac{H_0(s_i)\Delta s_i}{2}:\right)\right] \end{aligned} \quad (2)$$

where :: is the Lie operator [6] ($:f:g=\partial_{\mathbf{r}}f\cdot\partial_{\mathbf{p}}g-\partial_{\mathbf{p}}f\cdot\partial_{\mathbf{r}}g$), and T is the "time-ordering" symbol. Since the H_0 corresponds to the linear motion, $\exp(-:H_0:\Delta_s)$ can be written with a linear transfer matrix. Since $H_{\rm sc}$ does not contain the canonical momentum, $\exp(-:H_{\rm sc}:\Delta s)(\mathbf{r},\mathbf{p}) = (\mathbf{r},\mathbf{p}-\partial_{\mathbf{r}}H_{\rm sc}\Delta s)$. Hence, the last expression of Eq. (2) is solved exactly. Higher order symplectic integrators can also be obtained by slightly modifying Eq. (2) [7].

In order to reduce the calculation time of the space–charge interaction ($\propto N^2$), a periodic boundary condition for longitudinal direction is used [8]. When ions of charge $q=Ze$ are put at position $(s,r)=(0,0),(\pm L,0),(\pm 2L,0),\ldots,$ the electro-static potential in the region $|s|<L/2$ is

$$U_{\rm sc}(s,r) = \frac{1}{4\pi\varepsilon_0}\left(\frac{q}{\sqrt{s^2+r^2}} + \frac{2q}{L}\int_0^\infty \frac{J_0(kr/L)\cosh(ks/L)-1}{\exp(k)-1}{\rm d}k\right) \quad (3)$$

where J_0 is the Bessel function of 0th order. The longitudinal and transverse forces are obtained by partial differentials of the potential. The integrals in the forces are numerically calculated as functions of s/L and r/L, and used in the program as table values.

The momentum after every passage of electron cooling (EC) is approximated as

$$p_z\to(1-\eta_\ell)p_z,\quad p_x\to(1-\eta_{\rm t})p_x,\quad p_y\to(1-\eta_{\rm t})p_y \quad (4)$$

where η_ℓ and $\eta_{\rm t}$ are the longitudinal and the transverse cooling strengths, respectively.

3. Simulations of ESR experiments

The simulation code is applied to two ESR experiments [2,3].

First, one-dimensional crystallization experiment [2] is simulated. In the experiment, anomalous momentum spread reduction of the beam was observed when the number of ions in the ring was less than 10^3-10^4, depending on the ion species and the cooling strength by EC. The typical cooling rate is approximately 10–100 Hz for the longitudinal direction and 1–10 Hz for the transverse direction [4], which correspond to $\eta_\ell\approx 10^{-4}-10^{-5}$ and $\eta_{\rm t}\approx 10^{-5}-10^{-6}$, respectively. Since a simulation run with these values takes time (typically a few days with 833 MHz Alpha CPU) to reach an equilibrium, larger $\eta_\ell,\eta_{\rm t}$ were used. Fig. 1 shows the result for the 360 MeV/nucleon $^{197}Au^{79+}$ case when $\eta_\ell=\eta_{\rm t}=10^{-4}$. The phase transition from the random distribution to the 1D chain can be seen.

Fig. 2 shows the simulated momentum spread σ_p after 50,000 revolutions as a function of number of stored ions N for various cooling strengths. The phase transition is clearly observed. Below the transition, the momentum spreads are lower than the reality ($\sim 10^{-7}$), since constant cooling strengths are used. It is interesting that the threshold ion number increases as the transverse cooling rate decreases. This will be discussed in Section 4.

Next, heating rate experiment in ESR [3] is simulated. In the experiment with 390 MeV/nucleon $^{238}U^{92+}$, the electron current was switched on and off for time interval of 6.8 s. They observed that the low-intensity ($N=600$) cold beam heats up with a delay of about 1 s.

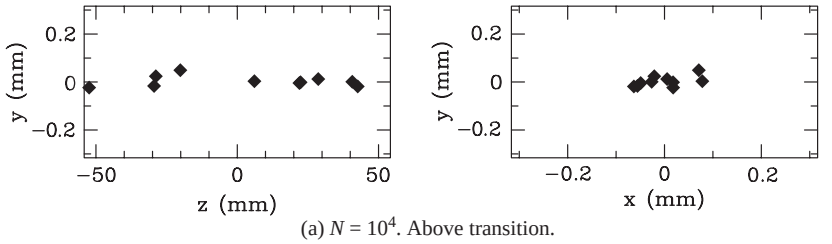

(a) $N = 10^4$. Above transition.

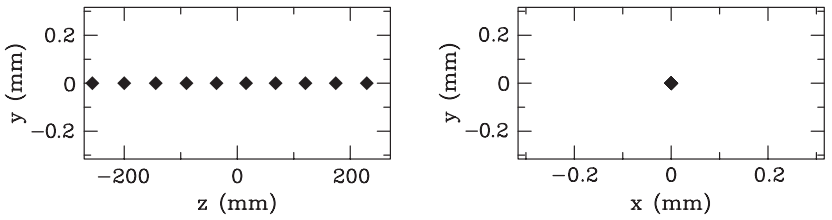

(b) $N = 2 \times 10^3$. Below transition.

Fig. 1. Simulated beam distributions for the ESR experiment. $\eta_\ell = \eta_t = 10^{-4}$. (a) $N = 10^4$. Above transition, (b) $N = 2 \times 10^3$. Below transition.

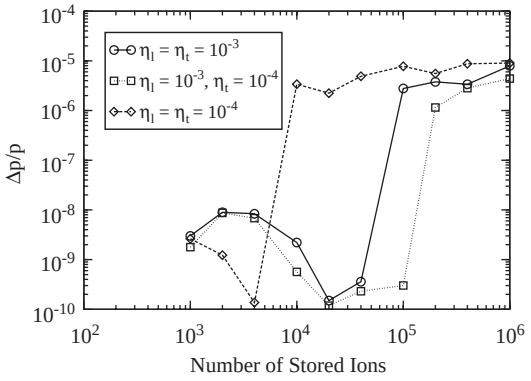

Fig. 2. Simulated momentum spread as a function of number of stored ions for various cooling strengths for 360 MeV/nucleon $^{197}Au^{79+}$ in ESR.

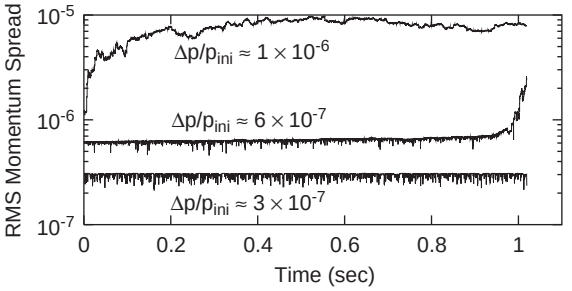

Fig. 3. Simulation of the experiment [3]. The parameters are $^{238}U^{92+}$, $N = 600$, $K = 390$ MeV/nucleon, $\varepsilon = 0.1$ πnm rad. Initial rms momentum spreads are $1 \times 10^{-6}, 6 \times 10^{-7}, 3 \times 10^{-7}$. Cooling is switched off.

This means the heating rate of cold beam is smaller than expected by the classical intra-beam scattering (IBS) theory [9,10].

The simulations are carried out with $\varepsilon = 0.1$ πnm rad beam consisting of 10 particles. In the simulation the cooling is always switched off. The result is shown in Fig. 3. With the initial momentum spread of $\Delta p/p_{\text{ini}} = 6 \times 10^{-7}$, the momentum spread suddenly increases after 1 s, which shows the similarity to the experiment. The symplectic integrator should be effective because the numerical error does not seem to build-up in 1 s for $\Delta p/p_{\text{ini}} = 3 \times 10^{-7}$ case.

4. Conditions for obtaining 1D crystalline state

Hasse and Schiffer [11] defined a dimensionless linear density as

$$\lambda_{\text{ion}} = \left(\frac{3N^3 r_{\text{ion}}}{8\pi^2 Q^2 C \gamma_0^5 \beta_0^2} \right)^{1/3} \tag{5}$$

where C and Q are the circumference and the betatron tune, respectively, to classify the ordered states ($0<\lambda_{\rm ion}<0.709$: 1D chain, $0.709<\lambda_{\rm ion}<0.964$: zig–zag,…). Transverse coherent tune of the μth mode $Q_\mu(\mu=0,1,\ldots,N-1)$ for the 1D crystalline state is

$$\frac{Q_\mu^2}{Q^2}=1-\frac{4\lambda_{\rm ion}^3}{3}\sum_{l=1}^{\infty}\frac{1-\cos(2\pi(Q_\mu+\mu)l/N)}{l^3} \tag{6}$$

which is plotted in Fig. 4.

It can be seen that the coherent tunes decrease as the line density increases. From the figure it can be guessed that if the normalized density is above 0.709 (2D or 3D crystalline state region), the coherent tunes are almost spread between 0 and the bare tune. So, for making 2D or 3D crystalline states, bare tune per super-periodicity should be less than 0.25 in order to keep any coherent mode away from fourth-order resonance. This is a hard condition for lattice design. For obtaining 1D state ($\lambda_{\rm ion}<0.709$), the condition is less severe. In this case, linear density should be lower than a threshold value where the smallest coherent tune hit some resonance. By assuming that the coherent tune shift should be less than 0.25, N should be less than, for 360 MeV/nucleon $^{197}Au^{79+}$ in ESR

$$N_{\rm sc}=\left(\frac{4\pi^2QC\gamma_0^5\beta_0^2}{7\zeta(3)r_{\rm ion}}\right)^{1/3}=3.9\times10^6 \tag{7}$$

where $\zeta(3)=1.2020569\ldots$, is the Riemann zeta function of 3. This condition does not give strict limitation to the lattice structure.

In the ESR case $\lambda_{\rm ion}=1.1\times10^{-3}$ when $N=10^4$, which means that the phase transition occurs in the 1D chain region. In this case, the phase transition is determined by the balance of the EC and the heating by IBS. According to a simplified classical IBS theory [12], the longitudinal heating rate

$$\frac{1}{T_p}\approx\frac{\sqrt{\pi}r_{\rm ion}^2cN(\log)}{8\gamma_0^3\varepsilon_x^{3/4}\varepsilon_y^{3/4}C\sigma_p^2\bar\beta_x^{1/4}\bar\beta_y^{1/4}}\propto\varepsilon^{-3/2}\sigma_p^{-2} \tag{8}$$

where (log) is the Coulomb log factor, increases as the momentum spread decreases. But when the momentum spread becomes low enough, the ion motion in the particle rest frame is restricted to small harmonic vibrations around an ordered arrangement. In this case, the IBS heating rate should be nearly zero [13].

Two phases can be distinguished by the reflection condition [14,15] that colliding two ions do not cross each other longitudinally. This condition can be roughly obtained from Eq. (1). When the two particles are colliding, the Hamiltonian of the relative longitudinal motion of them will be approximated as

$$H\approx\frac{p_z^2}{2\gamma_0^2}+\frac{2r_{\rm ion}}{\gamma_0^2\beta_0^2}\frac{1}{\sqrt{2\sigma_\perp^2+\gamma_0^2z^2}} \tag{9}$$

where $\sigma_\perp$ is the transverse beam size. The first and second terms on the right-hand side correspond to the kinetic and potential energies, respectively. Before the collision, two particles are separated with $z\approx C/N$, and the momentum difference is $p_z\approx\sqrt{2}\sigma_p$. Then they start to collide. But, if the potential energy at $z\approx0$ is large enough, they cannot cross each other. This condition gives the following relation

$$\begin{aligned}\sigma_p^2&<\frac{2r_{\rm ion}}{\beta_0^2}\left[\frac{1}{\sqrt{2\sigma_\perp^2}}-\frac{1}{\sqrt{2\sigma_\perp^2+\gamma_0^2(C/N)^2}}\right]\\&\approx\begin{cases}\dfrac{\sqrt{2}r_{\rm ion}}{\beta_0^2\sigma_\perp}, & \gamma_0C/N\gg\sigma_\perp\\[2ex]\dfrac{r_{\rm ion}\gamma_0^2C^2}{2\sqrt{2}N^2\beta_0^2\sigma_\perp^3}, & \gamma_0C/N\ll\sigma_\perp\end{cases}\end{aligned} \tag{10}$$

which is similar to Γ_2 condition in Ref. [15]. In this region, where the particles do not cross each other, the IBS heating rate should be smaller than the classical theory.

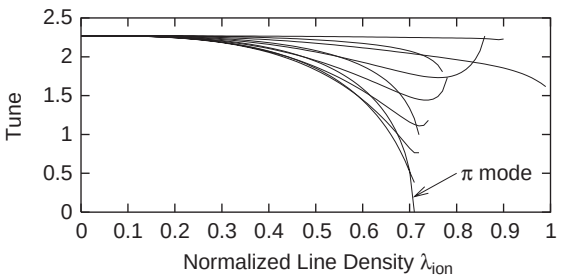

Fig. 4. Transverse coherent tune as a function of linear density.

During a cooling process, the ion beam distribution is going to transfer from the classical IBS region to the no-crossing region. From Eq. (10), the boundary of the two regions is $\sigma_p \propto \varepsilon^{-1/4}$, if $\gamma_0 C/N \gg \sigma_\perp$. Substituting this into Eq. (8), we obtain $T_p^{-1} \propto \varepsilon^{-1}$. This means that the high ε at the boundary may be more preferable. As a result, for a given longitudinal cooling rate, sometimes lower transverse cooling rate makes easier 1D crystallization. This is qualitatively consistent with the simulation results shown in Fig. 2.

In the 1D crystalline state the horizontal betatron oscillation modulates the longitudinal ion motion, and makes the momentum spread. From Eq. (1), the equations of longitudinal motion is written roughly as

$$\frac{\mathrm{d}z}{\mathrm{d}s} \approx \frac{p_z}{\gamma_0^2} - \frac{\sqrt{2}\sigma_\perp}{\rho} \sin\left(\frac{2\pi Q s}{C}\right)$$

$$\frac{\mathrm{d}p_z}{\mathrm{d}s} \approx \frac{r_{\mathrm{ion}}}{\gamma_0^3 \beta_0^2} \left\{ \frac{1}{(C/N+z)^2} - \frac{1}{(C/N-z)^2} \right\} \approx -\frac{4N^3 r_{\mathrm{ion}}}{\gamma_0^3 \beta_0^2 C^3} z. \quad (11)$$

The second term of the first equation drives the momentum spread. Consequently, the region

$$\sigma_p < \frac{2N^3 r_{\mathrm{ion}} \sigma_\perp}{\pi Q^2 \gamma_0^3 \beta_0^2 C^2} \quad (12)$$

is prohibited as a crystalline state. This phenomenon can be seen qualitatively in the simulations in Ref. [16].

5. Conclusion

A molecular dynamics simulation code using a second-order symplectic integral is developed. This code is applied to ESR experiments for 1D crystalline state, and the simulations reproduce the experiments quantitatively well. The theoretical maximum number of stored ions in 1D state is determined by the coherent tune shift. But the actual number is much smaller than the theory because of the low cooling rate. In some cases, the lower transverse cooling rate gives larger threshold.

References

[1] T. Katayama, et al., MUSES Conceptual Design Report, 2000.
[2] M. Steck, et al., Phys. Rev. Lett. 77 (1996) 3803.
[3] R.W. Hasse, M. Steck, Proceedings of the 2000 European Particle Accelerator Conference, Vienna, 2000, p. 274.
[4] M. Steck, et al., Proceedings of the 1993 Particle Accelerator Conference, 1993, p. 1738.
[5] J. Wei, X.P. Li, A.M. Sessler, Proceedings of the 1993 Particle Accelerator Conference, 1993, p. 3527.
[6] E. Forest, Beam Dynamics, A New Attitude and Framework, Harwood, Netherlands, 1998.
[7] H. Yoshida, Phys. Lett. A 150 (1990) 262.
[8] V.V. Avilov, Solid State Commun. 44 (1982) 555.
[9] A. Piwinski, Proceedings of the Ninth International Conference on High Energy Accelerators, 1974, p. 405.
[10] J.D. Bjorken, S.K. Mtingwa, Part. Accel. 13 (1983) 115.
[11] R.W. Hasse, J.P. Schiffer, Ann. Phys. 203 (1990) 419.
[12] K.L.F. Bane, Proceedings of the 2002 European Particle Accelerator Conference, Paris, 2002, p. 1443.
[13] Y. Shobuda, K. Yokoya, Phys. Rev. E 65 (2002) 026502.
[14] R.W. Hasse, Phys. Rev. Lett. 90 (2003) 204801.
[15] I. Meshkov, et al., RIKEN-AF-AC-34, 2002.
[16] A. Smirnov, et al., Nucl. Instr. and Meth. A, (2004) these proceedings.